Molecular Biology of the Cell
Vol. 12, 2195–2206, 2001

Null Mutants of the *Neurospora* Actin-related Protein 1 Pointed-End Complex Show Distinct Phenotypes

In Hyung Lee,* Santosh Kumar,† and Michael Plamann†§

*Department of Foods and Nutrition, Kookmin University, 861-1, Chongnung-dong, Songbuk-gu, Seoul 136-702, Korea; †School of Biological Sciences, University of Missouri-Kansas City, Kansas City, Missouri 64110-2499

Submitted October 26, 2000; Revised March 27, 2001; Accepted April 30, 2001
Monitoring Editor: Ted Salmon

Dynactin is a multisubunit complex that regulates the activities of cytoplasmic dynein, a microtubule-associated motor. Actin-related protein 1 (Arp1) is the most abundant subunit of dynactin, and it forms a short filament to which additional subunits associate. An Arp1 filament pointed-end–binding subcomplex has been identified that consists of p62, p25, p27, and Arp11 subunits. The functional roles of these subunits have not been determined. Recently, we reported the cloning of an apparent homologue of mammalian Arp11 from the filamentous fungus *Neurospora crassa*. Here, we report that *N. crassa ro-2* and *ro-12* genes encode the respective p62 and p25 subunits of the pointed-end complex. Characterization of Δ*ro-2*, Δ*ro-7*, and Δ*ro-12* mutants reveals that each has a distinct phenotype. All three mutants have reduced in vivo vesicle trafficking and have defects in vacuole distribution. We showed previously that in vivo dynactin function is required for high-level dynein ATPase activity, and we find that all three mutants have low dynein ATPase activity. Surprisingly, Δ*ro-12* differs from Δ*ro-2* and Δ*ro-7* and other previously characterized dynein/dynactin mutants in that it has normal nuclear distribution. Each of the mutants shows a distinct dynein/dynactin localization pattern. All three mutants also show stronger dynein/dynactin-membrane interaction relative to wild type, suggesting that the Arp1 pointed-end complex may regulate interaction of dynactin with membranous cargoes.

INTRODUCTION

Cytoplasmic dynein is a multisubunit, microtubule-associated force-producing enzyme required for the transport of various organelles, establishment of the mitotic spindle, and movement of chromosomes (Hirokawa, 1998; Steinberg, 1998; Allan, 1996; Karki and Holzbaur, 1999; Sheetz, 1999; Seiler *et al.*, 1999). Dynactin, an additional multisubunit complex that partially copurifies with dynein, has been proposed to link cytoplasmic dynein with membranous organelles and is also required for increased processivity of the dynein motor along microtubules (Allan, 1996; Schroer, 1996; Schroer *et al.*, 1996; Holleran *et al.* 1996; King and Schroer, 1999). The most abundant subunit of dynactin is actin-related protein 1 (Arp1) that forms a short (37 nm) filament (Schafer *et al.*, 1994). Certain cargoes have been proposed to link with dynein/dynactin through interaction of the Arp1 filament with a membrane-associated spectrin-like cytoskeleton (Holleran *et al.*, 1996).

Two distinct multisubunit subcomplexes associate with the Arp1 filament: a projecting shoulder/side arm complex and an Arp1 pointed-end complex. The shoulder/side arm complex consists of p150^{Glued}, dynamitin (p50), and p24 subunits and has been shown to mediate interaction of dynactin with dynein through contacts between p150^{Glued} and dynein IC (Karki and Holzbaur, 1995; Vaughan *et al.*, 1995; Waterman-Storer *et al.*, 1995; Echeverri *et al.*, 1996). The Arp1 pointed-end complex consists of p25, p27, p62, and Arp11 (Schafer *et al.*, 1994; Eckley *et al.*, 1999). The p25, p27, and p62 subunits contain predicted cargo-binding motifs and have been proposed to function in dynactin-membrane interaction, whereas the predicted structure of Arp11 suggests that it functions as an Arp1 pointed-end cap (Minke, Kumar, Lee, and Plamann; unpublished data; Eckley *et al.*, 1999). The p62 subunit has been shown to have Arp1 pointed-end–binding activity, and it may also play a role in linking dynein and dynactin to the cortical cytoskeleton (Garces *et al.*, 1999).

The Arp1 pointed-end subunits identified in mammals are evolutionarily conserved because homologous proteins are present in metazoans as diverse as *Drosophila* and *Caenorhabditis elegans* (Eckley *et al.*, 1999). In contrast, Arp1 pointed-end subunits are not found in the unicellular yeast *Saccharomyces cerevisiae*. Yeast dynein/dynactin participates in the formation of the mitotic spindle and the distribution of nuclei into mother and daughter cells; however, yeast dynein/dynactin are not required for microtubule-dependent

§Corresponding author. E-mail address: plamannm@umkc.edu.

transport of membranous organelles (Eshel *et al.*, 1993; Li *et al.*, 1993; Yeh *et al.*, 1995; Inoue *et al.*, 1998a, b). The lack of both dynein/dynactin-dependent endomembrane trafficking and conserved Arp1 pointed-end subunits in yeast provides support for the hypothesis that this subcomplex plays a role in the interaction of dynein/dynactin with membranous cargoes that are transported along microtubules (Eckley *et al.*, 1999).

In contrast to yeast, dynein/dynactin has been shown to be required for both nuclear movement and microtubule-dependent retrograde transport of membranous organelles in the filamentous fungus *Neurospora crassa* (Seiler *et al.*, 1999). Many *N. crassa* (ropy) mutants have been identified that are defective in dynein/dynactin function, and some of these *ro* genes have been found to encode subunits of the Arp1 pointed-end complex. We recently showed that the *N. crassa ro-7* gene encodes an apparent homologue of Arp11 (Minke, Kumar, Lee, and Plamann; unpublished data; Eckley *et al.*, 1999), and a partial sequence of the *N. crassa ro-2* gene revealed that it encodes a protein with significant identity to mammalian p62 (Vierula and Mais, 1997; Eckley *et al.*, 1999; Garces *et al.*, 1999). The availability of *N. crassa* genes encoding subunits of the Arp1 pointed-end complex makes it possible to use a genetic approach to examine the roles of each of the Arp1 pointed-end complex subunits in the association of dynactin with membranes and the long-range transport of membranous organelles. In this report, we describe the isolation of the *ro-2* and *ro-12* genes, encoding the respective p62 and p25 subunits of the dynactin Arp1 pointed-end complex. We present here a comparative analysis of mutants defective in three of the four Arp1 pointed-end complex subunits (*ro-2* [p62], *ro-7* [Arp11], and *ro-12* [p25]). We found that all three mutants have stronger dynactin-membrane interaction and are defective for vesicle transport and vacuole distribution. The *ro-2* and *ro-7* mutants have a severe nuclear distribution defect that is typical of most dynein/dynactin mutants; however, the *ro-12* mutant is unusual in that it has normal nuclear distribution. Our results suggest distinct functions for each of the subunits of the Arp1 pointed-end complex.

MATERIALS AND METHODS

Strains, Growth Conditions, and Genetic Techniques

The *N. crassa* wild-type (74-OR23–1A; FGSC 987) and *ro-1*(B15) (FGSC4352) strains were obtained from the Fungal Genetic Stock Center, Department of Microbiology, University of Kansas Medical Center, Kansas City, KS. Strains deleted for the *ro-2* and *ro-12* genes are described in the text, and strains deleted for *ro-3* and *ro-7* genes have been described previously (Minke, Kumar, Lee, and Plamann; unpublished data; Tinsley *et al.*, 1996). Media, growth conditions, and sexual crosses were done with the use of standard procedures (Davis and de Serres (1970). DNA-mediated transformations were carried out as described by Vollmer and Yanofsky, 1986), and where appropriate, media were supplemented with hygromycin B at 200 μg/ml. Mycelia were harvested from wild type grown for 18 h and from ropy mutants grown for 24 h in liquid media inoculated with 1×10^6 conidia/ml. The mycelia were harvested by filtration, frozen in liquid nitrogen, and kept at −80°C until use.

Isolation of ro-2 *and* ro-12 *Genomic Clones and DNA Sequence Analysis*

Sib selection was used to identify cosmid clones from the Orbach/Sachs cosmid library (Fungal Genetic Stock Center) which complement the *ro-2* and *ro-12* mutants (Vollmer and Yanofsky, 1986). *N. crassa* ropy mutants grow as slowly spreading colonies with curled hyphal growth (Garnjobst and Tatum, 1967; Tinsley *et al.*, 1996), and complementation results in restoration of straight hyphal growth and rapid radial expansion of individual colonies. To localize DNA containing the *ro-2* and *ro-12* genes, the respective complementing cosmid clones were digested separately with various restriction endonucleases and the digested DNAs were used to transform the *ro-2* and *ro-12* mutants. Restriction endonucleases that cut within insert sequences of the cosmid clones, but did not inactivate complementing activity, were used to subclone the *ro-2* and *ro-12* genes. DNA sequencing was performed with the use of an ABI PRISM Dye Terminator Cycle Sequencing Core Kit (Perkin Elmer-Cetus, Foster City, CA). GenBank searches were performed at the National Center for Biotechnology Information (Bethesda, MD), with the use of the BLAST network service (Altschul *et al.*, 1997). Sequence comparisons were done with the use of the MacVector program (Oxford Molecular Group PLC, Oxford, UK).

Disruption of the N. crassa ro-2 *and* ro-12 *Genes*

Plasmids were constructed that contain the respective *ro-2* and *ro-12* genes disrupted by a Hyg^r marker which confers resistance to the cytotoxin hygromycin B. The *ro-2* disruption plasmid was constructed by replacing a 997-bp *Sph*I-*Kpn*I fragment of the *ro-2* structural gene with a 2.6-kbp *Sph*I-*Kpn*I fragment containing the *trpC-hph* gene. The *ro-12* disruption plasmid was constructed by replacing a 495-bp *Msc*I-*Kpn*I fragment of the *ro-12* structural gene with a 2.6-kbp *Sph*I-*Sma*I fragment containing the *trpC-hph* gene. *N. crassa* strains disrupted for *ro-2* or *ro-12* genes were constructed by integrative transformation as described previously (Tinsley *et al.*, 1996). Disruptions of the *ro-2* and *ro-12* genes were verified by Southern analysis with the use of DNA from three independent null mutants (Lee, Kumar, and Plamann, unpublished results).

Microscopy

N. crassa hyphal and colony morphologies were determined by placing agar plugs containing actively growing hyphae at the center of plates and incubating at 25°C for 16–24 h. Hyphae were observed with the use of an SXE42 stereoscope (Olympus, New Hyde Park, NY), and pictures were taken with the use of Kodak Technical Pan black and white film (ASA set at 100; Kodak, Rochester, NY). In vivo movements of organelles were analyzed in colonies growing on slides with the use of computer-enhanced video microscopy as described previously (Seiler *et al.*, 1999). Care was taken to use only actively growing hyphae. Immunofluorescence microscopy was conducted as described by Tinsley *et al.* (1996). In brief, conidia were inoculated onto small pieces (0.5 × 0.5 cm) of Immobilon polyvinylidene difluoride membrane (Millipore, Bedford, MA) placed on sucrose minimal agar media and the plates were incubated at 25°C overnight. The filters were then quick-frozen in liquid propane, subjected to low temperature fixation, slowly warmed to room temperature, and then rehydrated with a final transfer into a phosphate buffer (100 mM, pH 7.0). Wild-type samples were digested as described by Minke *et al.* (1999a). Samples of ropy mutants were not digested but incubated in blocking solution (phosphate buffer with 1% bovine serum albumin) for 15 min. Samples were used for either RO1/RO3 immunolocalization or 4′,6-diamidino-2-phenylindole (DAPI) nuclear staining as described by Tinsley *et al.* (1996). Vacuole distribution was determined as described by Seiler *et al.* (1999) with modifications. Conidia (1×10^6/ml) were inoculated into 10 ml of glucose minimal medium and cultures were incubated for 12 h at 25°C. Cell Tracker Blue (Molecular Probes, Eugene, OR) was added

to final concentration of 10 μM, and hyphae were examined and photographed after 30 min of further incubation.

Antibody Production, Immunoprecipitation, and Immunoblotting

Anti-RO1 antibody and anti-RO3 antibody were produced as described by Minke *et al.* (1999b). Anti-RO2 antibodies were increased by expressing hybrid RO2 proteins in *Escherichia coli*, injecting the respective proteins into rabbit, and collecting antiserum. For the construction of expression vectors, an *Sal*I- *Nru*I fragment internal to the *ro-2* structural genes was cloned into vector pGEX-3x (Amersham Pharmacia Biotech, Piscataway, NJ). RO2-GST fusion protein was purified with the use of the Bulk GST Purification Module (Amersham Pharmacia Biotech) as described by Grieco *et al.* (1992). To maintain fusion protein solubility, dithiothreitol was added to a 5 mM final concentration before sonication of *E. coli* cells. Purified fusion protein was cut by factor X to separate RO2 and GST polypeptides. The resultant RO2 peptide was used to raise anti-RO2 antibodies in rabbits (Stratagic Biosolutions, Ramona, CA).

Immunoprecipitation was performed as previously described with some modifications (Beckwith *et al.*, 1998; Kumar *et al.*, 2000a). Cell extracts were diluted in NET-gel buffer (1:2), incubated with primary antibody (affinity-purified anti-RO3 antibodies or anti-RO2 antiserum, 10 μl each), and then incubated with protein A Sepharose (100 μl). The immunoprecipitant was collected by centrifugation, rinsed twice with wash buffer, and resuspended in 50 μl of phosphate-buffered saline and 20 μl of 4× sample buffer. The solubilized proteins were analyzed by SDS-PAGE (10%).

For immunoblotting, proteins resolved by SDS-PAGE were electroblotted onto a nitrocellulose membrane (Schleicher & Schuell, Keene, NH) and then probed with anti-RO1, anti-RO3, or anti-RO2 antibodies at 1:1000 dilution. Goat anti-rabbit immunoglobulin G secondary antibody conjugated to alkaline phosphatase was used at a 1:15,000 dilution (Promega, Madison, WI). Western blot processing was performed as described (Promega).

Sucrose Gradient Fractionation

High-speed (100,000 × *g*) cell extracts were made with 0.5 g of mycelia as described previously (Paschal *et al.*, 1991; Kumar *et al.*, 2000b). Samples of cell extracts (1 ml) were fractionated with the use of 5–20% sucrose gradients as described before (Paschal *et al.*, 1991; Kumar *et al.*, 2000b). After centrifugation at 120,000 × *g* for 16 h in an SW41 rotor (Beckman, Fullerton, CA), 0.5-ml fractions were removed starting at the bottom of the tubes. Proteins contained in each fraction were precipitated with trichloroacetic acid and analyzed by Western blotting. All operations were performed at 4°C.

Measurement of Dynein ATPase Activity

Dynein ATPase was isolated primarily as described by Kumar *et al.* (2000b). Mycelia (1.0 g) were resuspended in 2.5 ml of extraction buffer and cell extracts were prepared. Cell extracts (4 mg) were loaded onto a pre-equilibrated CL-4B S200 column and appropriate fractions containing cytoplasmic dynein were collected (fraction volumes, 28–37 ml). These fractions were assayed for ATPase activity as described before (Kumar *et al.*, 2000b). RO1 and RO3 proteins were detected in the isolated fractions by SDS-PAGE followed by Western blotting. All operations were performed at 4°C.

Dynein/Dynactin Membrane-binding Assay

Frozen mycelia (0.5 g each) were suspended in 1.5 ml of extraction buffer (EB) and the hyphae were ground with zirconium beads with the use of a mortar and pestle. Cell debris and zirconium beads were removed by centrifugation at 5000 × *g* for 10 min. Crude cell extracts were cleared by centrifugation at 28,000 × *g* for 10 min. Supernatant (0.5 ml) was incubated with 100 or 200 mM KCl (to remove loosely bound proteins from the membrane surface) for 60 min, overlaid over a 7.5% sucrose cushion (0.2 ml in EB), and then centrifuged at 100,000 × *g* in a Beckman Ti 100.3 rotor for 45 min to pellet down membranous organelles and membrane-associated proteins. The supernatant was desalted with the use of a Sephadex gel filtration column NAP (Amersham Pharmacia Biotech, Piscataway, NJ). The pellet was washed in 0.3 ml of 7.5% sucrose in EB and centrifuged at 100,000 × *g* for 45 min. The pellet was then resuspended with desalted supernatant (0.5 ml), incubated for 60 min, overlaid over a 7.5% sucrose cushion (0.2 ml in EB), and recentrifuged at 100,000 × *g* for 45 min. The pellet obtained from high-speed centrifugation was resuspended to the same volume as the supernatant. Samples (60 μl) from each supernatant and pellet were analyzed by SDS-PAGE, and RO1 and RO3 proteins were detected by Western blotting.

Membrane floatation experiments were done as described by Niclas *et al.* (1996). In brief, high-speed (100,000 × *g*) membrane pellets were resuspended in 2 M sucrose in EB (1 ml) and then layered above a 2 M sucrose/EB (1 ml) layer and below 1.4 M and 0.25 M sucrose/EB layers (1.5 ml each). Membranes were isolated at the 1.4 M/0.25 M sucrose interface after centrifugation at 260,000 × *g* for 120 min in an MS 50 rotor. Fractions (1 ml) were collected from the bottom of the tube and 60 μl from each fraction was analyzed by SDS-PAGE followed by Western blotting. All operations were performed at 4°C.

Fractionation of Membranous Organelles

N. crassa membranes were fractionated with the use of a procedure described for fractionation of yeast organelles (Walworth *et al.*, 1989). Frozen mycelia (3 g) were suspended in sorbitol-triethanolamine (TEA) lysis buffer (TEA 10 mM, pH 7.2, 0.8 M sorbitol, 1 mM EDTA, 1 mM dithiothreitol, and protease inhibitors; 1 mM phenylmethylsulfonyl fluoride, 10 μg/ml leupeptin, 10 μg/ml TAME (Nα-p-tosyl-L-arginine methyl ester), 1 μg/ml pepstatin A, and 10 μg/ml soybean trypsin inhibitor;). Zirconium beads were added, and mycelia were ground with the use of a mortar and pestle. Membranous organelles were isolated by centrifuging low-speed cell extracts at 100,000 × *g*, as described above in sorbitol-TEA buffer. The membrane fraction present in pellet (P100) was resuspended in 0.6 ml of sorbitol-TEA lysis buffer and microcentrifuged for 1 min to remove insoluble materials and protein aggregates. Sephacryl S-1000 (obtained from Sigma, 1.5- × 45-cm column) was pre-equilibrated with sorbitol-TEA lysis buffer and contained the same protease inhibitor cocktail used during extraction. The solubilized pellet containing membranes was loaded on to a pre-equilibrated column, and material was eluted over a 6-h period at a flow rate of 15 ml/h. The first 27 ml were collected together and then individual 3-ml fractions were collected. Fractions obtained from the S-1000 column were examined to measure the concentration of protein, phospholipid, RO1, and RO3. All operations were performed at 4°C.

RESULTS

ro-2 and ro-12 *Encode Arp1 Pointed-End Complex Subunits of Dynactin*

ro-2 and *ro-12* are among 23 complementation groups of ropy mutants that display a characteristic curled hyphal growth morphology (Garnjobst and Tatum, 1967; Bruno *et al.*, 1996.). With the use of a sib-selection protocol, cosmid clones X20H5 and G15E6 were isolated that complement the *ro-2* and *ro*-12 mutants, respectively (see MATERIALS AND METHODS). Examination of DNA sequence data indicates that the *ro-2* structural gene consists of a 634-codon open reading frame interrupted by a 65-bp intron. Previously, the *ro-2* gene was cloned and predicted to

encode a 710-amino acid polypeptide (Vierula and Mais, 1997). This predicted polypeptide contained an additional 173 amino acids at the N terminus and lacked 97 amino acids at the C terminus relative to our sequence. Additional information supports our interpretation of *ro-2* gene structure. First, cutting the *ro-2* plasmid with the restriction enzyme *Cla*I, located 275 bp upstream of our putative start codon and within sequences predicted previously to encode the N terminus of RO2, does not abolish the ability to complement a *ro-2* mutant. Second, sequences immediately downstream of the predicted *ro-2* start codon aligned well with putative homologues (Figure 1A; Lee, Kumar, and Plamann, unpublished results). Third, comparison of sequence information revealed a previous sequencing error that resulted in a loss of 97 residues from the predicted C terminus. The GenBank accession numbers for the *ro-2* and *ro-12* sequences are AF264758 and AF264759, respectively.

RO2 and RO12 show significant matches to the p62 and p25 subunits of the dynactin Arp1 pointed-end complex, respectively (Figure 1; Altschul *et al.*, 1997; Eckley *et al.*, 1999). Whereas the overall sequence homology between RO12 and p25 is high (38% identity), the overall similarity between RO2 and p62 is relatively low with only 18% identity to rat p62. In addition, *N. crassa* RO2 differs from p62 in that it contains several insertions resulting in a larger polypeptide (634 vs. 460 amino acids; Figure 1A). As described by Vierula and Mais (1997), a LIM domain is found in RO2 (residues 85–158), and this motif is also present in rat p62 (residues 51–118).

To further explore the possibility that RO2 represents the *N. crassa* p62 subunit of dynactin we used immunoprecipitation and sucrose gradient fractionation to determine whether RO2 is physically associated with either the dynein or dynactin complexes. Our results show that RO3 ($p150^{Glued}$) coimmunoprecipitates with RO2 when anti-RO2 antibody is used (Figure 2A). Similarly, RO2 coimmunoprecipitates with RO3 when anti-RO3 antibody is used (Figure 2A). Preimmune sera did not precipitate either RO2 or RO3 proteins. The high level of RO2 protein observed after immunoprecipitation with anti-RO2 antibodies vs. anti-RO3 antibodies suggests that under these conditions not all RO2 protein is associated with the dynactin complex. In contrast, similar amounts of RO3 are observed after immunoprecipitation with either antibody, suggesting that all RO3 is incorporated into the dynactin complex. This observation is consistent with previous work that showed that RO3 is degraded if it is not part of the dynactin complex (Minke *et al.*, 1999b).

We showed previously that *N. crassa* dynactin fractionates at ~15 S on sucrose gradients (Kumar *et al.*, 2000b). Here we fractionated dynactin from wild type and the Δ*ro-2* mutant, and RO1 (dynein heavy chain), RO2, and RO3 ($p150^{Glued}$) proteins were detected from sucrose gradient fractions by immunoblotting. The results showed that RO2 cofractionated with RO3 from wild type, and the fractionation pattern of dynactin, but not dynein, was slightly affected in the Δ*ro-2* mutant (Figure 2B). These results further support the sequence data suggesting that RO2 represents the *N. crassa* p62 subunit of the dynactin complex.

ro-2 and ro-12 *Null Mutants Are Viable and Have Curled Hyphal Growth*

To determine the phenotype of *ro-2* and *ro-12* null mutants, and whether these genes are essential, we constructed strains containing gene knockouts in which a segment of DNA spanning the predicted ATG translation initiation codon and a large part of the structural gene was replaced with DNA containing a Hyg^r-selectable marker (Cullen *et al.*, 1987); see MATERIALS AND METHODS). We successfully isolated homokaryotic strains disrupted for *ro-2* and *ro-12*, indicating that they are not essential for viability. The disruption strains also generate viable spores when crossed with wild type, again indicating the nonessential nature of the *ro-2* and *ro-12* genes. The Δ*ro-2* and Δ*ro-12* mutants display a curled hyphal growth phenotype typical of other dynein/dynactin null mutants (Lee, Kumar, and Plamann, unpublished results; Plamann *et al.*, 1994).

RO2 and RO7, but Not RO12, Are Required for Normal Nuclear Distribution

All previously described *ro* mutants defining genes encoding cytoplasmic dynein or dynactin subunits were found to have a distinctive nuclear distribution defect (Plamann *et al.*, 1994; Tinsley *et al.*, 1996; Minke *et al.*, 1999a). We found that *ro-2* and *ro-7* null mutants have a nuclear distribution defect typical of *ro-1* (dynein heavy chain) and *ro-3* ($p150^{Glued}$) null mutants (Figure 3; Plamann *et al.*, 1994; Tinsley *et al.*, 1996). However, the *ro-12* null mutant has normal nuclear distribution (Figure 3). The *ro-12* mutant represents one of four ropy complementation groups that have the typical ropy hyphal growth phenotype but normal or nearly normal nuclear distribution (Bruno *et al.*, 1996).

RO2, RO7, and RO12 Are Required for Vesicle Transport and Vacuole Distribution

Recently, video-enhanced contrast microscopy was used to examine vesicle trafficking in wild-type *N. crassa* and cytoplasmic dynein heavy chain (*ro-1*), dynactin $p150^{Glued}$ (*ro-3*), and conventional kinesin null mutants (Seiler *et al.*, 1999). In cytoplasmic dynein and dynactin null mutants, retrograde transport of organelles was virtually eliminated (>98% reduction), and there was accumulation of vacuoles at hyphal tips. The high concentration of vacuoles at hyphal tips was presumed to be a consequence of disrupting retrograde transport of organelles targeted to the vacuole system and the subsequent fusion of these static organelles with vacuole precursors located in tip regions (Seiler *et al.*, 1999). To determine whether subunits of the Arp1 pointed-end complex are also required for retrograde organelle movement, we examined vesicle transport and vacuole distribution in the *ro-2*, *ro-7*, and *ro-12* null mutants. We found that all three Arp1 pointed-end complex mutants are defective in vesicle trafficking as described previously for the dynein and dynactin null mutants (Lee, Kumar, and Plamann, unpublished results). In addition, as with the dynein and dynactin null mutants, there is clustering of vacuoles at hyphal tips in these three mutants (Figure 4).

Figure 1. Predicted amino acid sequences of *N. crassa* RO2 and RO12. (A) Alignment of the predicted amino acid sequence of *N. crassa* RO2 with p62 from rat and worm (*C. elegans*). (B) Alignment of the predicted amino acid sequence of *N. crassa* RO12 with p25 from mouse. Hyphens that interrupt sequences indicate gaps that were introduced to maximize the alignment. Dark and light shaded boxes indicate identical and similar amino acids, respectively.

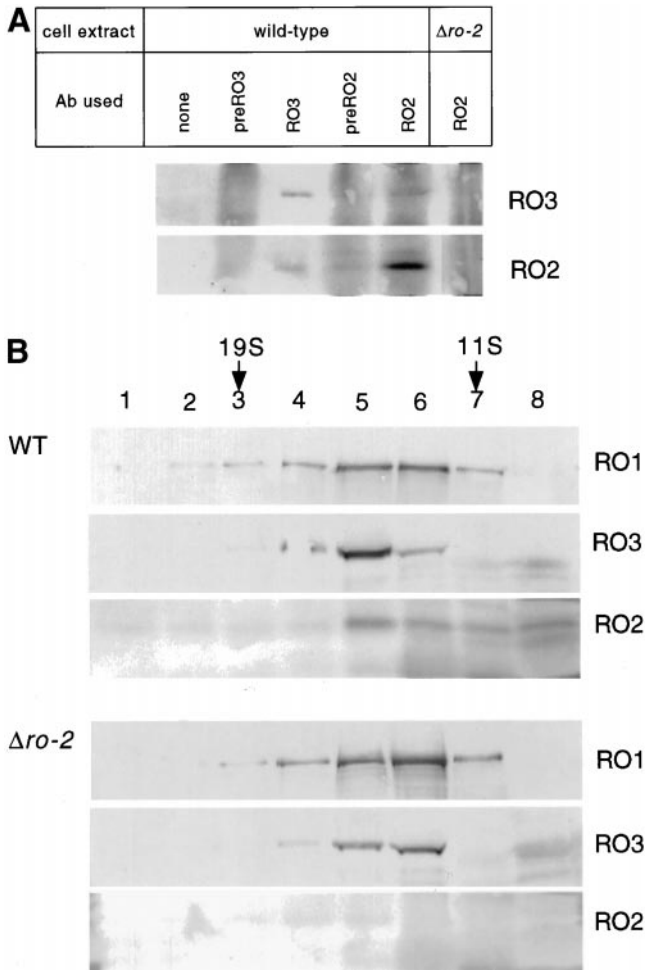

Figure 2. Association of *N. crassa* RO2 with RO3 ($p150^{Glued}$). (A) RO2 and RO3 were immunoprecipitated in separate experiments with the use of anti-RO2 and anti-RO3 antibodies, respectively. Immunoprecipitants were resolved by SDS-PAGE, and RO2 and RO3 proteins were detected by Western blotting. The cell extracts and antibodies (antibody) used in these experiments are indicated above the immunoblot. (B) Cell extracts from wild type (WT) and Δ*ro-2* were fractionated by centrifugation on 10-ml 5–20% linear sucrose gradients. Fractions (500 μl) were collected from the bottom of each tube (labeled lanes 1 through 8), and proteins were concentrated by trichloroacetic acid fractionation and then subjected to SDS-PAGE. RO1 (dynein heavy chain), RO2, and RO3 were detected by Western blotting. Sedimentation standards were thyroglobulin (19S), catalase (11S), and alcohol dehydrogenase (5S).

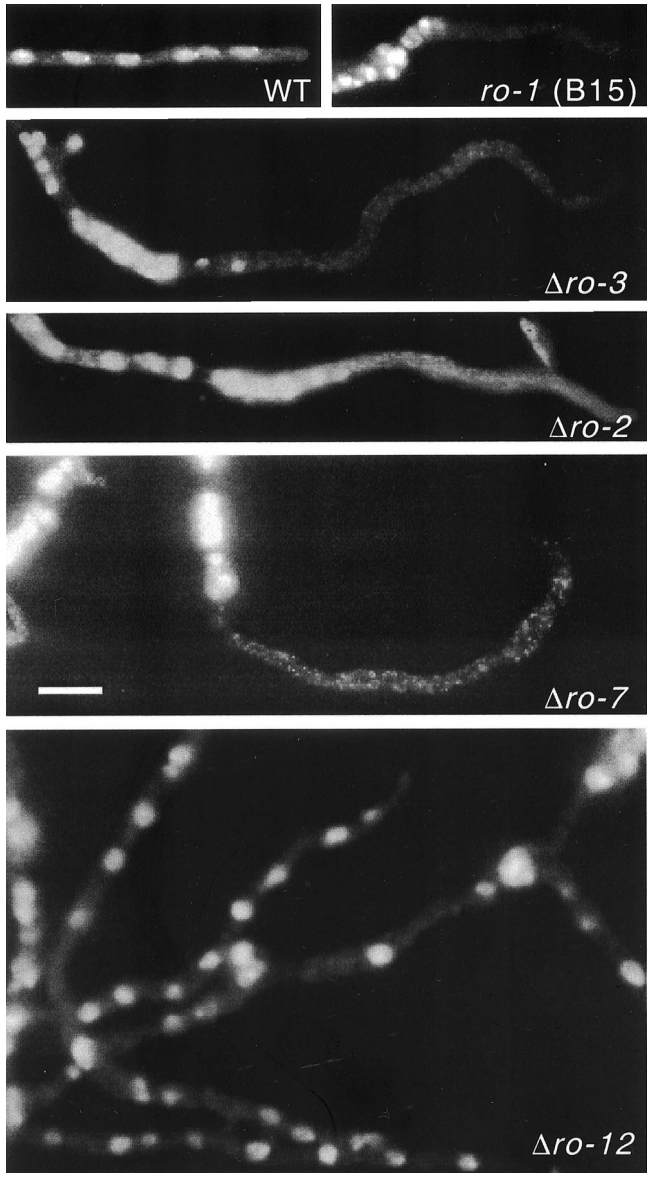

Figure 3. The effect of Arp1 pointed-end null mutations (Δ*ro-2*, Δ*ro-7*, and Δ*ro-12*) on nuclear distribution relative to wild type (WT) and the dynein heavy chain [*ro-1*(B15)] and dynactin $p150^{Glued}$ (Δ*ro-3*) null mutants. DAPI staining for nuclear localization was performed as described in MATERIALS AND METHODS. Bar, 5 μm.

Arp1 Pointed-End Complex Mutants Show Distinct Cytoplasmic Dynein and Dynactin Localization Patterns

Previous immunolocalization experiments with the use of affinity-purified antibodies to cytoplasmic dynein heavy chain (RO1) and $p150^{Glued}$ of dynactin (RO3) showed that both proteins exhibit a punctate cytoplasmic staining pattern with a concentration at hyphal tips in a wild-type strain of *N. crassa* (Figure 5; Minke *et al.*, 1999a)). In ~50% of the well-stained hyphal tips of wild type, we observe RO1 present in one or two spots or short 2- to 3-μm-long streaks at hyphal tips (Minke *et al.*, 1999a). In a dynactin null mutant (Δ*ro-3*), RO1 localization is still observed as a light punctate staining throughout the cytoplasm with an increase in staining at hyphal tips, but there are no spots or short streaks of RO1 at hyphal tips as there are in wild type (Minke *et al.*, 1999a).

We examined dynein (RO1) and dynactin (RO3) localization in *ro-2* and *ro-12* mutants to determine whether Arp1 pointed-end complex mutations have distinct dy-

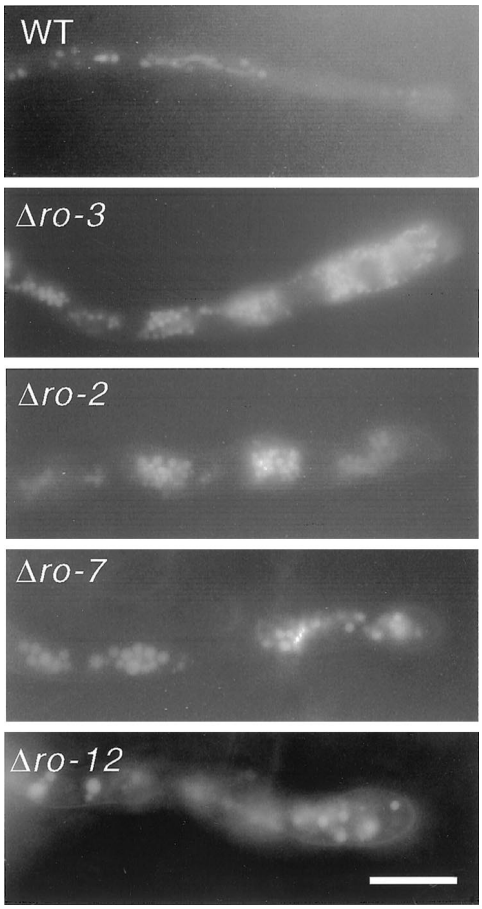

Figure 4. Vacuole distribution in Arp1 pointed-end null mutants (Δ*ro-2*, Δ*ro-7*, and Δ*ro-12*) relative to wild type (WT) and dynactin p150^{Glued} (Δ*ro-3*) null mutant. Staining for vacuoles was performed as described in MATERIALS AND METHODS. Bar, 5 μm.

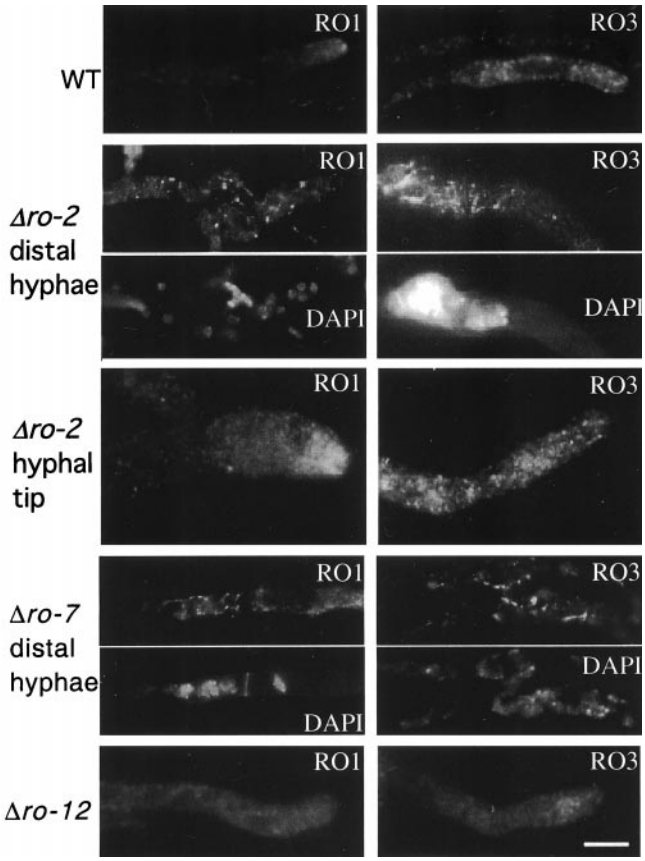

Figure 5. Immunolocalization of RO1 and RO3 in Arp1 pointed-end null mutations (Δ*ro-2*, Δ*ro-7*, and Δ*ro-12*) and wild type (WT). For Δ*ro-2* mutant, staining for RO1 and RO3 was from tip and distal regions, for Δ*ro-7* mutant, RO1 and RO3 staining was from only the distal region, and for Δ*ro-12*, RO1 and RO3 staining was from only hyphal tips. The *N. crassa* strains were labeled in the right side and proteins localized were labeled at the top of the figure. Samples were prepared for immunolocalization as described in MATERIALS AND METHODS. Bar, 5 μm.

nein localization patterns (Figure 5). We showed previously that in *ro-7* hyphae both RO1 and RO3 are absent from tip regions and localized as pronounced streaks and bright spots coincident with cytoplasmic microtubules associated with nuclear spindle pole bodies (SPBs; Minke, unpublished data). In contrast, we found that RO1 is primarily localized as a light punctuate stain throughout the cytoplasm in both the *ro-2* and *ro-12* deletion strains (Figure 5). There is a higher concentration of RO1 staining at newly formed tips of the Δ*ro*-2 mutant but not at newly formed tips of Δ*ro-12* (Figure 5). The RO3 punctate staining pattern observed in the *ro-2* and *ro-12* deletion strains is similar to the RO1 staining except we did not observe a concentration of RO3 at hyphal tips in these two mutants. In ~10% of the hyphae of the *ro*-2 mutant, we found RO1 and RO3 localized as bright spots and short streaks in regions of hyphae containing clustered nuclei in a pattern that is similar to Δ*ro-7* mutant (Figure 5; Minke, unpublished data). These results indicate that each Arp1 pointed-end complex mutation has a distinct effect on cytoplasmic dynein and dynactin localization patterns.

ro-2, *ro-7*, and *ro-12* Null Mutants Have Reduced Dynein ATPase Activity

The Δ*ro-2*, Δ*ro-7*, and Δ*ro-12* mutants have common defects in retrograde organelle transport; however, the distinct nuclear distribution and dynein localization phenotypes exhibited by these mutants suggests that the Arp1 pointed-end mutations may differ in their effects on the level of dynein ATPase activity or dynein/dynactin-membrane interaction. Recently, we showed that dynactin null mutations (i.e., mutants lacking either p150^{Glued} or Arp1) result in a 85–90% reduction in dynein ATPase activity (Kumar *et al.*, 2000b). Given the normal nuclear distribution observed in the Δ*ro-12* mutant, one might predict that this mutant has either normal dynein ATPase activity or significantly higher dynein ATPase activity than dynactin null mutants and other dynactin mutants with defective nuclear distribution. Similarly, the accumulation of dynein and dynactin at the minus ends of microtubules in the *ro-7* mutant (Minke, unpublished data) suggests that the dynein motor might be con-

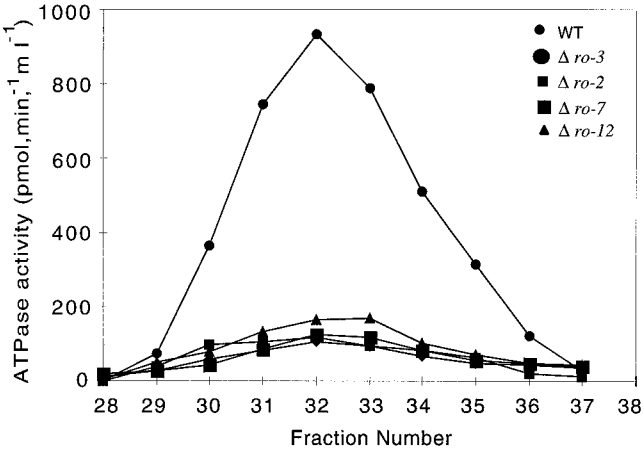

Figure 6. Dynein ATPase activity in wild type (WT) and Δ*ro-3*, Δ*ro-2*, Δ*ro-7*, and Δ*ro-12* mutants. Cell extracts from each strain were fractionated with the use of a Sepharose CL-4B (bed volume, 100 ml) column, and fractions volume from 28th to 37th were assayed for ATPase activity (see MATERIALS AND METHODS). Data are representative of three independent experiments. The values are within the range of 5% for each assay from three independent preparations.

stitutively active and show higher dynein ATPase relative to ropy mutants where dynein/dynactin are distributed in a punctate manner. Therefore, dynein ATPase activity was determined from wild type, a dynactin null control strain (Δ*ro-3*; lacking p150^{Glued}), and the Δ*ro-2*, Δ*ro-7*, and Δ*ro-12* mutants. A gel filtration protocol was used to fractionate extracts from each strain (see MATERIALS AND METHODS; Kumar *et al.*, 2000b), and fractions containing dynein were assayed for ATPase activity and the amount of dynein heavy chain (RO1). The abundance of RO1 was the same from all the mutants relative to wild type (Lee, Kumar, and Plamann, unpublished results). Surprisingly, we found that dynein ATPase activity was reduced in each of the dynactin mutants to the level observed in the Δ*ro-3* dynactin null mutant (i.e., ~10–15% of the level observed in wild type; Figure 6). As with the Δ*ro-3* dynactin null mutant, the reduced dynein ATPase activity observed in the Arp1 pointed-end mutants could be stimulated by the addition of microtubules and was increased to near wild-type levels by treatment with λ protein phosphatase before ATPase activity measurement (Lee, Kumar, and Plamann, unpublished results, Kumar *et al.*, 2000b).

Dynein/Dynactin-Membrane Interaction Is Stronger in All Arp1 Pointed-End Complex Mutants

Dynactin has been proposed to link membranous cargoes with dynein motor through contacts between the dynactin Arp1 filament and a spectrin-like cytoskeleton associated with the surface of membranous cargoes (Holleran *et al.*, 1996). The Arp1 pointed-end complex subunits p25, p27, and p62 have also been proposed to play a role in cargo binding (Eckley *et al.*, 1999). To investigate the role of pointed-end complex subunits in membrane binding, we examined dynein- and dynactin-membrane binding in the *ro-2*, *ro-7*, and *ro-12* null mutants relative to wild type. As controls for our membrane-binding studies, we examined the effects of the pointed-end mutations on the levels and sedimentation properties of dynein and dynactin. We found that all three Arp1 pointed-end complex mutations did not alter the level of RO1 (dynein heavy chain; Figure 7A) or the sedimentation properties of cytoplasmic dynein (Figure 2B; Lee, Kumar, and Plamann, unpublished results). However, the three Arp1 pointed-end mutations did have effects on dynactin. In the Δ*ro-12* mutant, the level of RO3 (p150^{Glued}) was reduced to ~75% of wild type, and in the Δ*ro-2* and the Δ*ro-7* mutants the level of RO3 was ~25% of wild type. Although the sedimentation coefficient of dynactin was not altered in the Δ*ro-12* mutant (Lee, Kumar, and Plamann, unpublished results), the sedimentation coefficient of dynactin did decrease slightly in both the Δ*ro-2* and the Δ*ro-7* mutants as predicted for dynactin complexes lacking these larger (62 and 71 kDa, respectively) subunits (Figure 2A; Minke, unpublished data).

High-speed centrifugation and membrane flotation were used to examine dynein- and dynactin-membrane interaction in wild type and the three mutants (see MATERIALS AND METHODS). Low-speed extracts were first prepared from each strain and subjected to high-speed centrifugation to obtain a crude estimate of the amount of membrane-associated dynein and dynactin (Figure 7B, lanes 1 and 2). We found that salts present in low-speed extracts interfered with dynein- and dynactin-membrane interaction; therefore, to obtain a more accurate determination of the amount of membrane-bound dynein and dynactin, we examined membrane binding in desalted extracts. First, we added KCl to low-speed extracts to a concentration of 100 mM (Figure 7B, lanes 3 and 4) or 200 mM (Figure 7B, lanes 5 and 6) before high-speed centrifugation to release all dynein and dynactin from the membrane. The supernatants containing both soluble and salt-released dynein and dynactin were then desalted by gel filtration, mixed with and without salt-washed pellets containing membranes, and then subjected to high-speed centrifugation (Figure 7B, lanes 7–10). Finally, flotation centrifugation was used to establish that pelleted dynein and dynactin represent complexes associated with membrane (Figure 7B, lanes 11 and 12).

Approximately 30% of the dynein and dynactin was pelleted from low-speed extracts of wild type (Figure 7B, lanes 1 and 2). Adding KCl to a concentration of 100 mM solubilized (i.e., released from membrane) all dynein and dynactin present in extracts of wild type (Figure 7B, lanes 3 and 4). Desalting extracts of wild type and mixing with salt-washed pellets before high-speed centrifugation resulted in pelleting of ~40% of dynein and dynactin (Figure 7B, lanes 9 and 10). High-speed centrifugation of desalted extracts from wild type without the addition of salt-washed pellet did not result in pelleting of dynein and dynactin (Figure 7B, lanes 7 and 8).

As with wild type, 40–50% of the dynein was pelleted from low-speed extracts of each of the pointed-end mutants; however, >70% of the dynactin pelleted from extracts of the Δ*ro-2* and the Δ*ro-7* mutants (Figure 7B, lanes 1 and 2). This increase in the fraction of membrane-associated dynactin relative to wild type may be due to the reduced pool of dynactin in these mutants (~25% of wild type; Figure 7A). Alteration of the relative ratios of dynein to dynactin in these mutants may be driving most of the dynactin into a

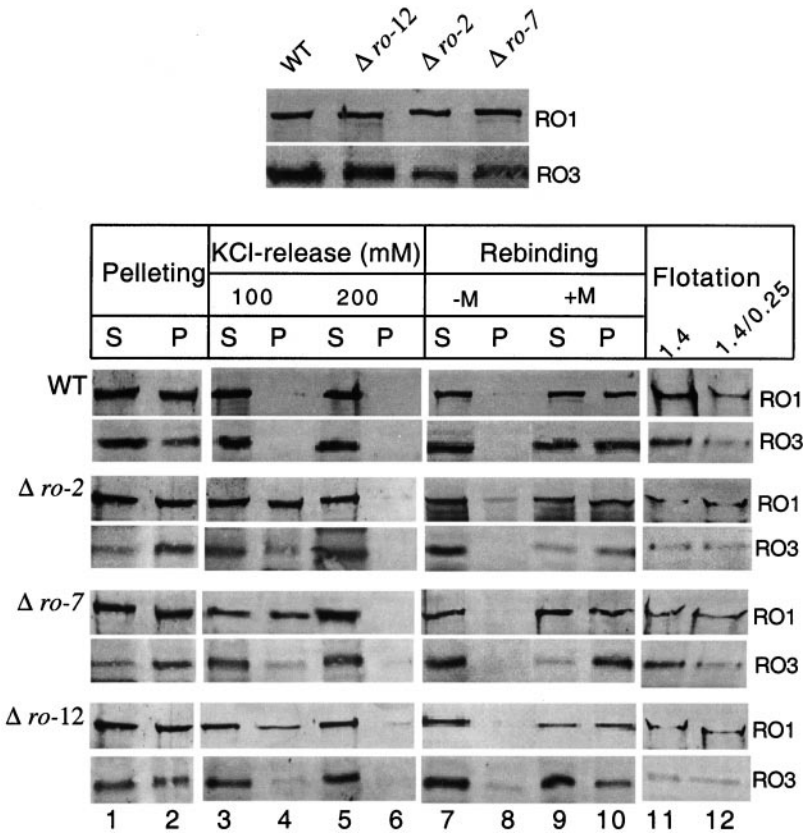

Figure 7. Dynein and dynactin membrane association in wild type (WT) and Arp1 pointed-end complex mutants. (A) The abundance of dynein (RO1) and dynactin (RO3) was determined by Western blotting of low-speed cell extracts from wild type, Δ*ro-12*, Δ*ro-2*, and Δ*ro-7*. (B) Dynein- and dynactin-membrane binding was determined by salt-dependent pelleting and membrane-flotation experiments (see MATERIALS AND METHODS). *N. crassa* strains used are labeled on the left, and the RO1 and RO3 proteins detected by immunoblotting are labeled on the right. Lanes 1 and 2 are supernatant and pellet, respectively, after high-speed (100,000 × *g*) centrifugation of low-speed cell extracts. Lanes 3 and 4 are supernatant and pellet, respectively, after 100,000 × *g* centrifugation of 100 mM KCl-treated low-speed cell extract. Lanes 5 and 6 are supernatant and pellet, respectively, after 100,000 × *g* centrifugation of 200 mM KCl-treated low-speed cell extract. Lanes 7 and 8 are supernatant and pellet, respectively, after 100,000 × *g* centrifugation of supernatant without the addition of pellet from lanes 5 and 6. Lanes 9 and 10 are supernatant and pellet, respectively, after 100,000 × *g* centrifugation of recombined desalted supernatant and pellet from lanes 5 and 6. Lanes 11 and 12 are 1.4 M sucrose and 1.4/0.25 M sucrose interface after flotation of membranes contained within the pellet fraction present in lane 10 (see MATERIALS AND METHODS). Rebinding experiments were conducted in either the absence (−M) or presence (+M) of membrane fraction.

membrane-bound state. In contrast to wild type, it was necessary to add KCl to a concentration of 200 mM to each of the extracts of the Arp1 pointed-end mutants before all the dynein and dynactin was released from membrane (Figure 7B, lanes 3–6). However, dynein- and dynactin-membrane interaction in the Δ*ro-12* mutant was more sensitive to salt relative to the Δ*ro-2* and Δ*ro-7* mutants. This finding suggests that dynein- and dynactin-membrane interaction is stronger in each of the Arp1 pointed-end mutants. After desalting of solublized dynein and dynactin from each of the mutants and mixing with salt-washed pellets before high-speed centrifugation, we found pelleting (i.e., restoration of membrane binding) of dynein and dynactin from each mutant (Figure 7B, lanes 9 and 10). As with wild type, high-speed centrifugation of desalted extracts lacking the addition of a salt-washed pellet results in all dynein and dynactin remaining in the soluble fraction (Figure 7B, lanes 7 and 8).

N. crassa dynein/dynactin are required for nuclear distribution and retrograde transport; therefore, it is likely that dynein/dynactin interacts with plasma membrane and with vesicles derived from the endocytic pathway (Valetti *et al.*, 1999). The stronger dynein- and dynactin-membrane interaction observed in the three Arp1 pointed-end mutants may be due to tighter binding of dynein and dynactin to its normal target membranes or the result of increased nonspecific membrane binding. To differentiate between these two possibilities, we fractionated membranes present in the high-speed pellets (P100s) and then determined the amounts of dynein and dynactin in each membrane fraction. The results from wild type showed that the dynein/dynactin fractionation profile is clearly distinct relative to the lipid profiles, suggesting that dynein binds to specific membrane organelle(s) (Lee, Kumar, and Plamann, unpublished results). The fractionation pattern of dynein and dynactin from the Δ*ro-2*, Δ*ro-7*, and Δ*ro-12* mutants was also not altered (Lee, Kumar, and Plamann, unpublished results). These results suggest that, although the three Arp1 pointed-end mutations result in tighter membrane binding, they do not change the specificity of dynein/dynactin-membrane interaction relative to wild type.

DISCUSSION

Dynactin has been proposed to act as a regulatory complex that directs and controls the transport activities of cytoplasmic dynein. The complex structure of dynactin has been suggested as necessary for its regulated interaction with dynein and the diverse array of cargoes transported by dynein. Recently, a distinct subcomplex of dynactin was identified that consists of Arp11, p62, p27, and p25 subunits and associates with the pointed-end of the Arp1 filament (Eckley *et al.*, 1999). The predicted structure of the Arp11 subunit suggests that it provides Arp1 pointed-end capping activity, whereas analysis of the primary sequences of the p62, p27, and p25 subunits has led to the hypothesis that these subunits function in the interaction with membrane (Eckley *et al.*, 1999). We have been conducting a large-scale

genetic analysis of dynein and dynactin in *N. crassa*, and we have defined the *ro-7*, *ro-2*, and *ro-12* genes as encoding the Arp11, p62, and p25 Arp1 pointed-end complex subunits, respectively (Minke, unpublished data; Plamann *et al.*, 1994; Bruno *et al.*, 1996.) The nonessential nature of *N. crassa* dynein/dynactin has allowed us to conduct a comparative analysis of null mutants that lack specific subunits of the Arp1 pointed-end complex. The work presented here identifies for the first time a dynactin subunit (p25) that is not required for nuclear distribution, and we provide evidence that the Arp1 pointed-end complex is involved in regulating the interaction of dynactin with membrane.

Arp1 Pointed-End Complex and Nuclear Distribution

Until now, the defining characteristic of *N. crassa* dynein/dynactin mutants has been defective nuclear distribution (Plamann *et al.*, 1994; Bruno *et al.*, 1996; Minke *et al.*, 1999). However, we demonstrated previously that four of the 23 known complementation groups of *N. crassa* ropy mutants have normal nuclear distribution (Bruno *et al.*, 1996). This observation suggested that some dynein/dynactin subunits might function for targeting specific cargoes. Our finding that the p25 subunit of the Arp1 pointed-end complex is not required for nuclear distribution, but is required for retrograde vesicle trafficking, supports this hypothesis. Identification of the other three ropy genes with normal nuclear distribution may lead to the identification of additional dynein/dynactin subunits or dynein/dynactin regulators that function specifically in retrograde vesicle trafficking. The p27 subunit of the Arp1 pointed-end complex is closely associated with p25, making it likely that this subunit is encoded by one of these three uncharacterized ropy genes. It is possible that the other two uncharacterized ropy genes encode proteins required for regulated interaction of dynein and dynactin with membranous cargoes.

The requirement of the Arp11 and p62 subunits, but not p25, for normal nuclear distribution may be due to the decreased level of dynactin (25%) observed in the *ro-2* and *ro-7* mutants, (i.e., for nuclear distribution, >75% of the normal level of dynactin is required). Although we cannot rule out this possibility, we think it unlikely that an approximately threefold difference in dynactin levels observed between the *ro-12* mutant and the *ro-2* and *ro-7* mutants would result in such a drastic difference in the ability to distribute nuclei. It may be that the differences between these mutants are due primarily to the effects of the individual mutations on membrane binding. We have noted previously that nuclei appear to move by force generation on SPBs (Minke *et al.*, 1999a). This force could result from dynein/dynactin, associated with plasma membrane, pulling on microtubules linked to SPBs. Alternatively, dynein/dynactin associated with the nuclear membrane at SPBs may provide the motive force for the movement of nuclei along cytoplasmic microtubules. Regardless, if proper nuclear movement requires a dynamic interaction between dynein/dynactin and plasma or nuclear membrane (i.e., periodic binding and release of dynein/dynactin from membrane), then the tighter membrane binding observed in the *ro-2* and *ro-7* mutants, relative to wild type and the *ro-12* mutant, may be the reason that only these two Arp1 pointed-end complex mutants have defects in nuclear distribution.

The mechanism by which dynactin participates in nuclear distribution is unknown. Recently, we showed that dynein ATPase activity is reduced by 85–90% in dynactin null mutants relative to wild type, and this increased the possibility that the loss of nuclear distribution in dynactin null mutants might be due to a reduction in dynein ATPase activity and not the physical loss of dynactin (Kumar *et al.*, 2000a). However, the work presented here shows clearly that in the Δ*ro-12* mutant this reduced level of dynein ATPase is sufficient to carry out nuclear distribution and suggests a physical role for dynactin in nuclear movement. The ~85% reduction in dynein ATPase activity in the *ro-12* (p25) mutant relative to wild type suggests that only a small amount of dynein ATPase activity is required for nuclear positioning and that the majority of fungal cytoplasmic dynein functions in nonnuclear transport processes, including retrograde vesicle trafficking.

Arp1 Pointed-End Complex and Endomembrane Trafficking

An analysis of the sequences of the p62, p27, and p25 subunits of the Arp1 pointed-end complex has led to the prediction that these subunits interact with membrane (Eckley *et al.*, 1999), and one would assume that removal of these subunits would lead to either the elimination or reduction of dynactin-membrane interaction (Eckley *et al.*, 1999). Surprisingly, our analysis of mutants lacking the p62, p25, and Arp11 subunits indicates that the strength of dynactin-membrane interaction is not decreased but actually enhanced in the p62 and Arp11 null mutants and to a lesser extent in the p25 mutant as well. These results suggest that the Arp1 pointed-end complex is not required for dynactin-membrane binding but perhaps for the regulated interaction of dynactin with membranous cargoes. One possible reason for increased membrane-binding strength in these mutants is that the putative capping activity of the Arp1 pointed-end complex may provide the proper geometry to the Arp1 filament for regulated interaction with membranous cargoes. In the absence of the Arp1 pointed-end complex or a complete complex, the degree of structural freedom within the Arp1 filament is increased, allowing tighter binding to membrane-associated target protein, which in turn either slows or prevents the release of membranous cargo. The more severe membrane-binding defect in the p62 and Arp11 mutants relative to the p25 mutant may be because p62 and Arp11, which always copurify, provide the Arp1 filament pointed-end capping activity, whereas the associated p25 and p27 subunits may be responsible for regulating the proper geometry of the Arp1 filament through alteration of p62/Arp11 conformation. In support of this hypothesis, the geometry of actin filaments is known to be a malleable property because ADF/cofilin binding results in an increased twist of 5° per subunit of actin filament (for review see Bamburg *et al.*, 1999).

Alternatively, in the absence of Arp1 pointed-end subunits the length of the actin filament may be increased, and this would provide additional surface area to bind to multiple Arp1 filament-binding proteins associated with the surface of membranous cargoes. However, our sedimentation data indicate that the size of the dynactin complex is not greatly affected by the three Arp1 pointed-end complex mutations, and any increase in Arp1 filament length must be

relatively small. Arp1 polymerization has also been shown to be self-regulated with purified Arp1 forming filaments that are 52 nm in length (Bingham and Schroer, 1999). Therefore, it seems unlikely that a sufficiently long Arp1 filament could be generated to provide additional vesicle receptor-dynactin contacts.

Finally, the distinct localization patterns of dynein in Arp1 pointed-end mutants may be due to differences in dynein processivity and/or recycling. Recently, dynactin has been implicated in the processivity of the dynein motor (King and Schroer, 1999). Our previous results also suggested that dynein is activated by dynactin-dependent dephosphorylation at tip regions, and at the distal regions of hyphae, dynein is inactivated by a protein kinase that leads to release of cargo and recycling of the motor (Kumar *et al.*, 2000a). In the *ro-7* null mutant, dynein and dynactin are localized primarily at the minus-ends of microtubules (Minke, unpublished data), whereas in the *ro-12* null mutant both complexes show a uniform punctate localization pattern. The *ro-2* mutant shows a localization pattern that is intermediate between these two extremes. In the *ro-7* null mutant, it is likely that dynein is activated at hyphal tips by a phosphatase and then transports vesicles to distal regions where it gets inactivated by a kinase. However, the lack of Arp11 makes dynein/dynactin unable to release membranous cargo and recycle the motor. In the *ro-2* and *ro-12* null mutants, it is likely that membrane binding also occurs at tip regions; however, defects in processivity of the motors or increased recycling in these mutants, relative to the putative recycling block in the *ro-7* mutant, may be the cause of the different localization patterns. Additional work will be required to determine how subunits of the Arp1 pointed-end complex contribute to the binding and release of membranous cargoes, dynein/dynactin recycling, and motor processivity.

ACKNOWLEDGMENTS

We thank Kenneth Bruno for help with the cloning of the *ro-2* gene at the beginning, acknowledge Yi Zhou for his effort in making anti-RO2 antibody, and thank Drs. Seiler and Purnapatre for providing helpful comments. This work was supported by grant GM51217 from the National Institutes of Health.

REFERENCES

Allan, V. (1996). Motor proteins: a dynamic duo. Curr. Biol. *6*, 630–633.

Altschul, S.F., Madden, T.L., Schäffer, A.A., Zhang, J., Zhang, Z., Miller, W., and Lipman, D.J. (1997). Gapped BLAST and PSI-BLAST: a new generation of protein database search programs. Nucleic Acids Res. *25*, 3389–3402.

Bamburg, J.R., McGough, A., and Ono, S. (1999). Putting a new twist on actin: ADF/cofilins modulate actin dynamics. Trends Cell Biol. *9*, 364–370.

Beckwith, S.M., Roghi, C.H., Liu, B., and Morris, N.R. (1998). The "8-kD"cytoplasmic dynein light chain is required for nuclear migration and for dynein heavy chain localization in *Aspergillus nidulans*. J. Cell Biol. *143*, 1239–1247.

Bingham, J.B., and Schroer, T.A. (1999). Self-regulated polymerization of the actin-related protein Arp1. Curr. Biol. *9*, 223–226.

Bruno, K.S., Tinsley, J.H., Minke, P.F., and Plamann, M. (1996). Genetic interactions among cytoplasmic dynein, dynactin, and nuclear distribution mutants of *Neurospora crassa*. Proc. Natl. Acad. Sci. USA *93*, 4775–4780.

Cullen, D., Leong, S.A., Wilson, L.J., and Henner, D.J. (1987). Transformation of *Aspergillus nidulans* with the hygromycin-resistance gene hph. Gene *57*, 21–26.

Davis, R.H. and de Serres, F.J. (1970). Genetic and microbiological research techniques for *Neurospora crassa*. Methods Enzymol. *27A*, 79–143.

Echeverri, C.J., Paschal, B.M., Vaughan, K.T., and Vallee, R.B. (1996). Molecular characterization of the 50-kD subunit of dynactin reveals function for the complex in chromosome alignment and spindle organization during mitosis. J. Cell Biol. *132*, 617–633.

Eckley, D.M., Gill, S.R., Melkonian, K.A., Bingham, J.B., Goodson, H.V., Heuser, J.E., and Schroer, T.A. (1999). Analysis of dynactin subcomplexes reveals a novel actin-related protein associated with the Arp1 minifilament pointed end. J. Cell Biol. *147*, 307–320.

Eshel, D., Urrestarazu, L.A., Vissers, S., Jauniaux, J.-C., van Vliet-Reedijk, J.C., Planta, R.J., and Gibbons, I.R. (1993). Cytoplasmic dynein is required for normal nuclear segregation in yeast. Proc. Natl. Acad. Sci. USA *90*, 11172–11176.

Garces, J.A., Clark, I.B., Meyer, D.I., and Vallee, R.B. (1999). Interaction of the p62 subunit of dynactin with Arp1 and the cortical actin cytoskeleton. Curr. Biol. *9,* 1497–1500).

Garnjobst, L., and Tatum, E.L. (1967). A survey of new morphological mutants in *Neurospora crassa*. Genetics *57*, 579–604.

Grieco, F., Hay, J.M., and Hull, R. (1992). An improved procedure for the purification of protein fused with glutathione S-transferase. Biotechnique*s 13*, 556.

Hirokawa, N. (1998). Kinesin and dynein superfamily proteins and the mechanism of organelle transport. Science *279*, 519–526.

Holleran, E.A., Tokio, M.K., Karki, S., and Holzbaur, E.L.F. (1996). Centractin (ARP1) associates with spectrin revealing a potential mechanism to link dynactin to intracellular organelles. J. Cell Biol. *135*, 1815–1829.

Inoue, S., Yoder, O.C., Turgeon, B.G., and Aist, J.R. (1998a). A cytoplasmic dynein required for mitotic aster formation in vivo. J. Cell Sci. *111*, 2607–2614.

Inoue, S., Yoder, O.C., Turgeon, B.G., and Aist, J.R. (1998b). Role of fungal dynein in hyphal growth, microtubule organization, spindle pole body motility and nuclear migration. J. Cell Sci. *111*, 1555–1566.

Karki, S., and Holzbaur, E.L.F. (1995). Affinity chromatography demonstrates a direct binding between cytoplasmic dynein and the dynactin complex. J. Biol. Chem. *131*, 385–397.

Karki, S., and Holzbaur, E.L.F. (1999). Cytoplasmic dynein and dynactin in cell biology and and intracellular transport. Curr. Opin. Cell Biol. *11*, 45–53.

King, S.J., and Schroer, T.A. (1999). Dynactin increases the processivity of the cytoplasmic dynein motor. Nat. Cell Biol. *2*, 20–24.

Kumar, S., Lee, I.H., and Plamann, M. (2000a). Cytoplasmic dynein ATPase is regulated by dynactin-dependent phosphorylation. J. Biol. Chem. *275*, 31798–31804.

Kumar, S., Lee, I.H., and Plamann, M. (2000b). Two approaches to isolate cytoplasmic dynein ATPase from *Neurospora crassa*. Biochimie *82*, 229–236.

Li, Y.Y., Yeh, E., Hays, T., and Bloom K. (1993). Disruption of mitotic spindle orientation in a yeast dynein mutant. Proc. Natl. Acad. Sci. USA *90*, 10096–10100.

Minke, P.F., Lee, I.H., and Plamann, M. (1999a). Microscopic analysis of *Neurospora* ropy mutants defective in nuclear distribution. Fungal Genet. Biol. *28*, 55–67.

Minke, P.F., Lee, I.H., Tinsley, J.H., Bruno, K.S., and Plamann, M. (1999b). *Neurospora crassa ro-10* and *ro-11* genes encode novel proteins required for nuclear distribution. Mol. Microbiol. *32*, 1065–1076.

Niclas, J., Allan, V.J., and Vale, R.D. (1996). Cell cycle regulation of dynein association with membranes modulates microtubule-based organelle transport. J. Cell Biol. *133*, 585–593.

Paschal, B.M., Shpetner, H.S., and Vallee, R.B. (1991). Purification of brain cytoplasmic dynein and characterization of its *in vitro* properties. Methods Enzymol. *196*, 181–191.

Plamann, M., Minke, P.F., Tinsley, J.H., and Bruno, K.S. (1994). Cytoplasmic dynein and actin-related protein Arp1 are required for normal nuclear distribution in filamentous fungi. J. Cell Biol. *127*, 139–149.

Schafer, D.A., Gill, S.R., Cooper, J.A., Heuser, J.E., and Schroer, T.A. (1994). Ultrastructural analysis of the dynactin complex: an actin-related protein is a component of a filament that resembles F-actin. J. Cell Biol. *126*, 403–412.

Schroer, T.A. (1996). Structure and function of dynactin. Semin. Cell Biol. *7*, 321–328.

Schroer, T.A., Bingham, J.B., and Gill, S.T. (1996). Actin-related protein 1 and cytoplasmic dynein-based motility: what's the connection? Trends Cell Biol. *6*, 212–215.

Seiler, S., Plamann, M., and Schliwa, M. (1999). Kinesin and dynein mutants provide novel insights into the roles of vesicle traffic during cell morphogenesis in *Neurospora*. Curr. Biol. *9*, 779–785.

Sheetz, M.P. (1999). Motor and cargo interactions. Eur. J. Biochem. *202*, 19–25.

Steinberg, G. (1998). Organelle transport and molecular motors in fungi. Fungal Gen. Biol. *24*, 161–177.

Tinsley, J.H., Minke, P.F., Bruno, K.S., and Plamann, M. (1996). $p150^{Glued}$, the largest subunit of the dynactin complex, is nonessential in *Neurospora* but required for nuclear distribution. Mol. Biol. Cell *7*, 731–742.

Valetti, C., Wetzel, D.M., Schrader, M., Hasbani, M.J., Gill, S.R., Kreis, T.E., and Schroer, T.A. (1999). Role of dynactin in endocytic traffic: effects of dynamitin overexpression and colocalization with CLIP-170. Mol. Biol. Cell *10*, 4107–4120.

Vaughan, K.T., Vallee, R.B., Vaughan, K.T., and Vallee, R.B. (1995). Cytoplasmic dynein binds dynactin through a direct interaction between the intermediate chains and $p150^{Glued}$. J. Cell Biol. *131*, 1507–1516.

Vierula, P.J., and Mais, J.M. (1997). A gene required for nuclear migration in *Neurospora crassa* codes for a protein with cystein-rich, lim/ring-like domains. Mol. Microbiol. *24*, 331–340.

Vollmer, S.J., and Yanofsky, C. (1986). Efficient cloning of genes of *Neurospora crassa*. Proc. Natl. Acad. Sci. USA *83*, 4869–4873.

Walworth, N.C., Goud, B., Ruohola, H., and Novick, P.J. (1989). Fractionation of yeast organelles. Methods Cell Biol. *31*, 335–354.

Waterman-Storer, C.M., Karki, S., and Holzbaur, E.L.F. (1995). The $p150^{Glued}$ component of the dynactin complex binds to both microtubules and the actin-related protein centractin (Arp1). Proc. Natl. Acad. Sci. USA *92*, 1634–1638.

Yeh, E., Skibbens, R.V., Cheng, J.W., Salmon, E.D., and Bloom, K. (1995). Spindle dynamics and cell cycle regulation of dynein in the budding yeast *Saccharomyces cerevisiae*. J. Cell Biol. *130*, 687–700.